

FSW of aluminium alloy AlSi12

Varjenje s trenjem in mešanjem aluminijeve zlitine AlSi12

Damjan Klobčar^{1,*}, Aleš Nagode², Anton Smolej², Janez Tušek¹

¹Faculty of Mechanical Engineering, University of Ljubljana, Aškerčeva cesta 6, 1000 Ljubljana, Slovenia

²Faculty of Natural Sciences, Department of Materials and Metallurgy, University of Ljubljana, Aškerčeva cesta 12, 1000 Ljubljana, Slovenia

*Corresponding author. E-mail: damjan.klobcar@fs.uni-lj.si

Abstract

FSW of 4 mm thick casting aluminium alloy AlSi12 and dissimilar welding of AlSi12 with Al 99.5 in butt joint was done. A classical tool was used with tilt angle of 2°, tool rotation speed varied from 235 r/min to 1 180 r/min, welding speed between 71 mm/min to 450 mm/min and joint gap width from 0 mm to 0.5 mm. From the produced welds, samples for microstructure analysis were prepared for observation on a light microscope under the polarized light source. A Vickers micro-hardness was measured across the weld. Analysis of microstructure, hardness measurement and tensile test of FSW welds were done. A set of FSW welding parameters was determined at which acceptable welds were obtained. Dissimilar welding of AlSi12 with Al 99.5 is possible.

Key words: friction stir welding, aluminium alloy EN AW 4430A (AlSi12), microstructure, mechanical properties, dissimilar welding

Izvleček

V prekravnem spoju smo s trenjem in mešanjem varili 4 mm debelo pločevino iz aluminijeve zlitine AlSi12 ter AlSi12 z Al 99,5. Uporabili smo klasično orodje s čepom. Spreminjali smo hitrost varjenja orodja med 235 r/min in 1 180 r/min, hitrost varjenja pa je bila med 71 mm/min in 450 mm/min, nagibni kot orodja 2°, širina špranje pa 0 mm in 0,5 mm. Iz zvarov smo izdelali vzorce za analizo mikrostrukture ter merjenje natezne trdnosti. Mikrostrukturo vzorcev smo pregledali z optičnim mikroskopom v polarizirani svetlobi in izmerili trdoto po Vickersu. S parametrično analizo smo določili procesno okno varilnih parametrov, da lahko dobimo kakovostne zvarne spoje. Spajanje aluminijeve zlitine AlSi12 s čistim aluminijem Al 99,5 je mogoče.

Ključne besede: varjenje s trenjem in mešanjem, aluminijeva zlitina EN AW 4430A (AlSi12), mikrostruktura, mehanske lastnosti, varjenje različnih materialov

Introduction

One of the current trends and goals of transportation industry is to lower the green gas emissions, increase fuel economy and use renewable energy. This is partly achievable by a) reduction of car body weight, b) engine volume and weight downsizing, c) the use of hybrid engines and/or d) electric engines. Weight reduction could be achieved using materials with favorable weight to strength ratio (Al alloys, Mg alloys, high strength steels etc.). Especially in a production of hybrid engines there is a demand for heat exchangers, cooling units or other closed shapes products for cooling of electric components and other various purposes. These products have complex shape and needs to be light, produced in high series, with sharp dimensional tolerances, and with low production costs. This is easily done using high pressure die casting technology (HPDC). With the HPDC closed parts cannot be produced directly, but some sort of joining must be used. Screw fastening is time consuming and expensive. Adhesive bonding has limitations in strength at higher temperature. Arc welding (MIG) of castings is demanding due to lubrication of the molds during HPDC i.e. castings, which produces metal explosions during arc welding and pores in the weld, which can cause leaking. TIG welding is slightly easier, producing less porosity in the weld.

FSW is a promising technology for joining castings made of different casting alloys. The advantages of FSW are that a) a sound welds can be made (without pores), b) no material explosions are present due to absence of molten metal and c) no filler material and shielding gasses are needed. The disadvantage is the pricier weld due to higher investment cost, tools and clamping devices. A weldability of different casted aluminium alloys is studied, regarding microstructure and mechanical properties^[1-11]. Results showed that welding is possible, but there are the limitations regarding welding parameters. Optimization of welding parameters using Taguchi methods showed that the tool rotation speed has the highest influence of the strength of the weld and the second influencing parameter is welding speed^[12]. FSW welding of

dissimilar aluminium alloys is more demanding and has a smaller processing window.

The aim of the research was to analyze weldability of AlSi12 in die casted condition. Aluminium alloy AlSi12 has a good castability, machinability and strength and limited weldability using arc welding technique. It is resistant to chemically aggressive liquids, has a low melting temperature, and is good for producing thin-walled castings of complex geometry. FSW welding parameters i.e. tool rotation speed, welding speed and tilt angle have the influence on the formation of welding defects, weld apices appearance, microstructure and weld strength. The aim of this research is to discover the welding parameters providing weld microstructure without defects. FSW was done at tool rotation speed from 235–1180 r/min, welding speed from 71–450 mm/min and the tool tilt angle was held constant at 2°. Factors feed per revolution (*FPR*) and revolutions per feed (*RPF*) were introduced to get the better insight into the friction stirring process. The *RPF* gives the information about heat input per weld length. Miniature samples for tensile testing were prepared from the welds. Welds were examined under the light optic microscope and Vickers hardness was measured.

Materials and methods

Dimensions and chemical composition of workpieces

The standard EN AW 4430A (AlSi12) aluminium alloy with chemical composition in mass fractions according to the standard (0.55 % Mn, 10.5–13.5 % Si, 0.08 % Cu, 0.45–0.9 % Fe, 0.15 % Zn, 0.15 % Ti and the rest Al) in die casted state was used for testing. The workpiece dimensions were 160 mm × 55 mm × 4 mm. Physical and mechanical properties of the alloy were not determined but taken according to standard (Table 1)^[13].

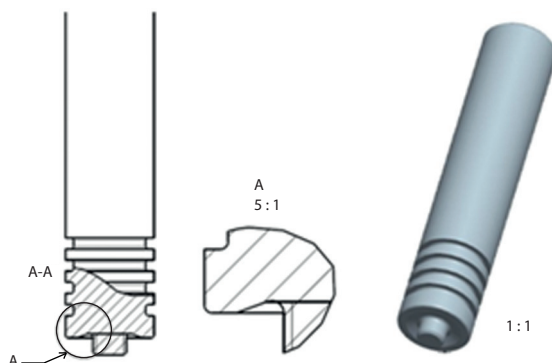
FSW tool

The FSW tool was made from standard EN 42CrMo4 steel^[14]. A basic FSW tool geometry was used with treaded pin 3.9 mm long (M6 × 1.5) and the concave shoulder

Table 1: Physical and mechanical properties of HPDC alloy AlSi12^[13]

Label	ρ (kg/m ³)	R_m (MPa)	$R_{p0.2}$ (MPa)	λ (W/m K)	T_{sol} (°C)	$T_{casting}$ (°C)
AlSi12	2 680	170–240	80–130	130–160	570–580	650–700

($\Phi = 16$ mm) for producing pressure under the tool shoulder (Figure 1). After machining the tool was surface quenched and tempered to get the surface hardness of 58 HRC.

**Figure 1:** FSW tool geometry.

Friction stir welding

A plan of experiments was prepared regarding capabilities of universal milling machine used (Prvomajska ALG 200). Different combinations of tool rotations and welding speeds were tested at constant tilt angle of 2°. The FSW tool rotated from 235 r/min to 1 180 r/min, and the welding speeds changed from 71 mm/min to 450 mm/min. Factor of feed per revolution (*FPR*) in mm/r and revolution per feed (*RPF*) in r/mm were introduced for better distinguishing between different welding parameters. The *FPR* varied from 60 mm/r to 1 620 mm/r. *RPF*, which represents the “frictional heat input” per weld length, was between 16.16–0.62 r/mm. A backing plate underneath the workpiece enabled the formation of pressure under the tool shoulder by preventing the aluminium alloy to flow away from the seam. The two workpieces were clamped in a vice.

Preparation of samples and welding

From the FSW welds a miniature tensile test samples were sectioned perpendicular to the welding direction, and a weld cross-sections for analysis of microstructure and macrostructure. Before sectioning the samples with water

jet, the workpiece surfaces were milled to remove weld underfill and toe flash.

The uniaxial tensile tests were done using computer controlled Zwick/Roell Z050 tensile testing machine. Measurements were done using Testexpert software. The strain was measured with extensometer directly on the sample.

The samples for analysis of microstructure and macrostructure were sectioned, grinded and polished. The samples for macrostructure analysis were etched using Keller reagent (1 125 ml HCl, 558 ml HNO₃, 200 ml HF and 1 500 ml H₂O) and the microstructure was analysed using a light optic microscope. Samples for microstructure analysis were anodizing with Baker’s reagent. The microstructure was examined using a light optic microscope under polarised light and with the digital camera for picture acquiring. A Vickers micro-hardness HV1 (load is 9.807 N) was measured across the welds.

Results and discussion

Dimensions and chemical composition of workpieces

Figure 2 shows the FSW weld apices. The end of the weld is indicated with a hole, which is a negative of the FSW tool pin. Visual assessment of the weld apices reveals smooth weld apices for *FPR* between 60 mm/r and 560 mm/r i.e. for *RPF* between 16.2 r/min and 1 r/mm (Figure 3). At sample 9 (Figure 2g) frictional heat input was the highest (*RPF* = 16.2 r/mm). At this sample a tool moved a bit too much into the workpiece, due to higher frictional heat input, which softened the material. At samples 3, 8, 1 and 2 (Figures 2f, e, d, and c) the *RPF* was between 11.3 r/mm and 1.78 r/mm and weld apices were smooth. When the tool speed increased to a 1 r/mm and 0.44 r/mm (Figures 2b, a) the heat input become smaller and weld apices become rough with the traces of material tearing.

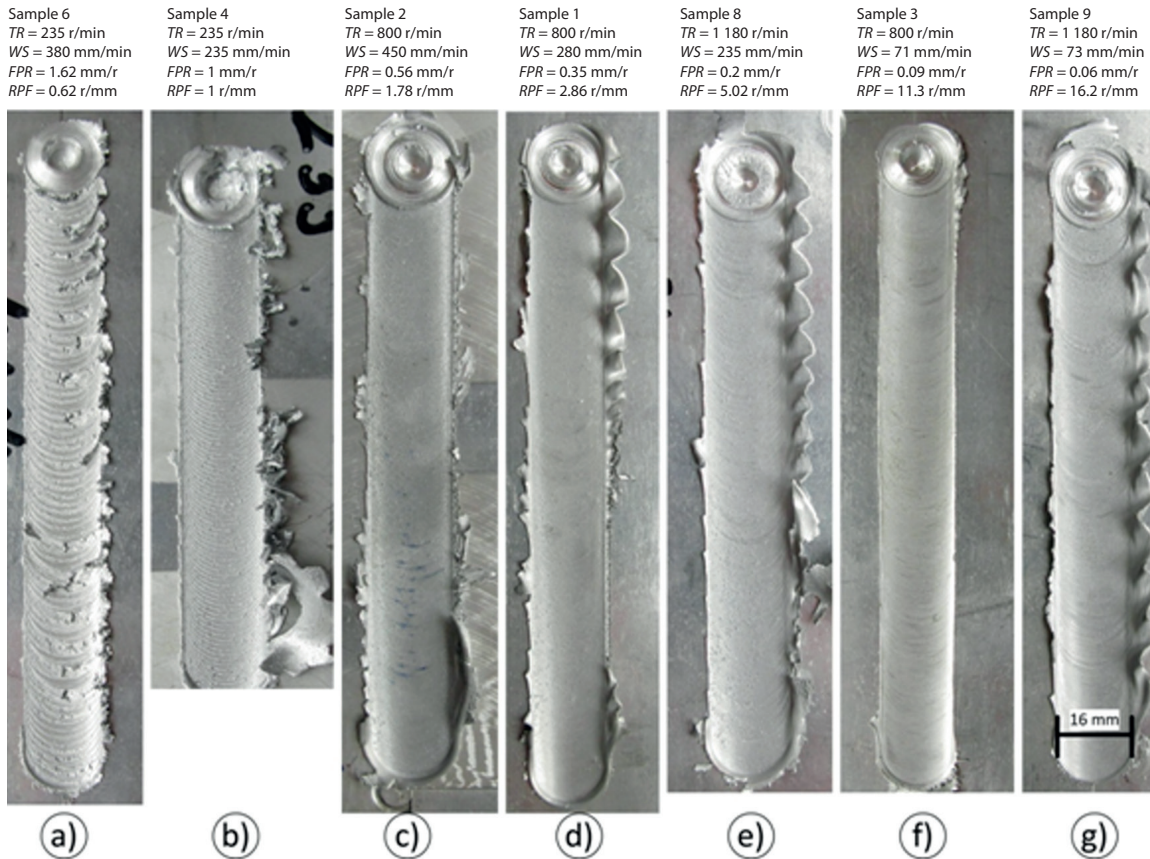


Figure 2: FSW weld apices produced with different parameters.

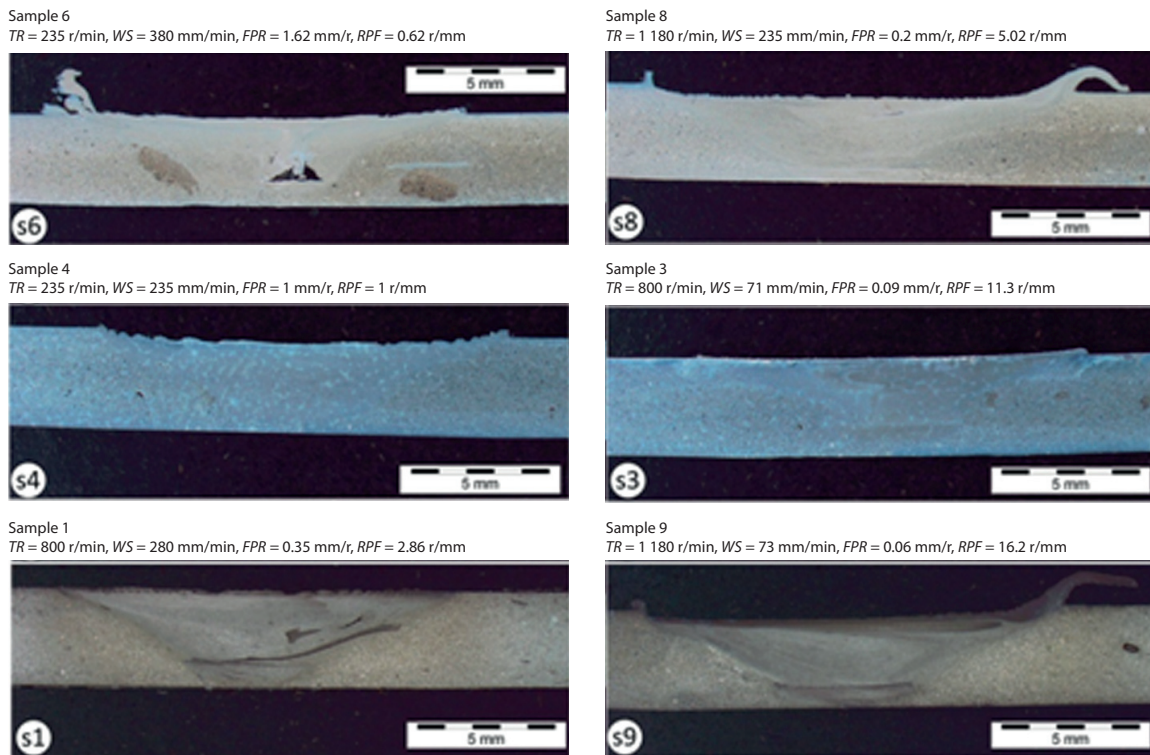
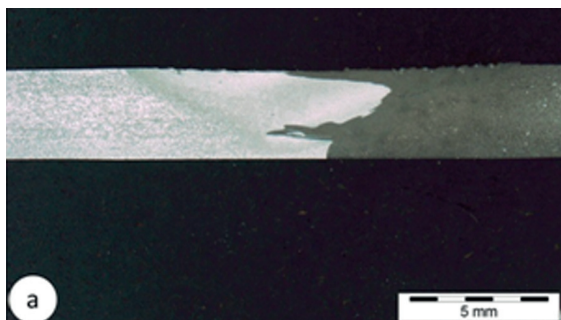


Figure 3: FSW weld macrostructure presented according to the heat input.

Weld microstructure

Macrographs of the selected FSW welds are shown on the Figure 3. The die casted base alloy had plenty of pores, which vanished in the weld. Figure 3 s6 presents the macrograph of sample 6, welded with the smallest frictional heat input ($RPF = 0.62$ r/mm). The “worm hole” i.e. “tunnelling” defect appears if welding is done with insufficient heat input or if welding force in the axial direction is not big enough. If heat input was higher than 1 rev/min no such defect was present. At samples s1 and s8 (Figure 3) a small cavity is present closer to the weld apices. The probable reason for that is insufficient tool penetration i.e. pressure under the tool shoulder or force in z-direction. Samples s4, s3 and s9 (Figure 3) represents quality weld without defect, except of small under-fill and toe flash, as a result of higher heat input. Figure 4 shows a macrostructure of two dissimilar welds obtained at a) RPF 1.25 r/mm with AlSi12 on the advancing side, and b) $RPF = 1.97$ r/mm with Al 99.5 on the advancing side. In both cases a quality weld, with good mixing

Sample 12
 $TR = 475$ r/min, $WS = 380$ mm/min, $FPR = 0.8$ mm/r, $RPF = 1.25$ r/mm



Sample 13
 $TR = 750$ r/min, $WS = 380$ mm/min, $FPR = 0.51$ mm/r, $RPF = 1.97$ r/mm

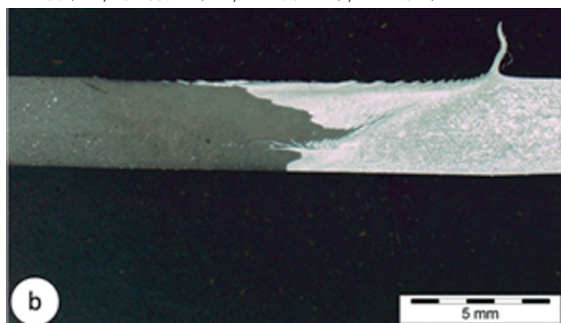


Figure 4: Dissimilar FSW weld between AlSi12 and Al 99.5: a) AS = AlSi12, b) AS = Al 99.5.

of both materials is obtained. The weld shows finer microstructure compared to either of the two base metals, and less porosity. Weld on Figure 4a was produced with less heat input and has no under-fill is present. At weld (Figure 4b) produced at higher heat input a toe flash is present at the advancing side of the weld due to higher heat input and better forming ability of the pure aluminum.

Figure 5 shows weld microstructure in the weld, HAZ and base alloy. The grain size at weld apices (Figures 5b, c) is very small due to vicinity of tool shoulder i.e. heat generation. Small sized grains are obtained across the whole weld (Figure 5a). At weld root material is not stirred to the bottom of the workpiece (Figure 5d). The oxide surface of contacting workpieces is clearly seen. Such oxide line/layer could present initiation site for cracking during loading or exploitation.

Hardness

The Vickers hardness HV1 was measured across the weld at the middle of the weld (2 mm below the surface) in the total distance of 26 mm. The hardness is shown for the samples 0, 7, 1 and 6 (Figure 6). The centre of the weld is shown with the “dash-dot” line and the advancing side of the weld is on the right side of the plot of the Figure 6. When welding with higher frictional heat input of 16.2 r/mm, the whole workpiece was heated above the temperature of recrystallization, where a grain growth occurs. The hardness was the lowest among all compared samples (≈ 80 HV1 in the base metal and HAZ, and 60 HV1 in the weld). When welding with optimal welding parameters (sample 7 and 1), the hardness across the weld was slightly higher (63–73 HV1) and was smaller than in the base alloy. A higher frictional heat input at the advancing side of the weld is resulting in a slightly lower hardness in the HAZ (≈ 75 HV1). When frictional heat input was very low (≈ 0.62 r/mm) weld hardness was 68 HV1.

At dissimilar weld (Figure 6 s13) with Al 99.5 on the advancing side hardness is decreasing to the softer Al 99.5, where hardness of 60 HV is obtained in the base metal.

Tensile properties

The tensile strength of the base alloy used for experimental workpiece was not measured, but taken from the literature data (Table 1). Yield strength of AISi12 aluminium alloy is between 80 MPa and 130 MPa and ultimate tensile strength between 170 MPa and 240 MPa (Table 1). Since a non-standard test specimens were used, the results could hardly be com-

pared with the results from the literature. The ultimate tensile strength of tensile test specimens was generally in the range of the base aluminium alloy. When welding with high heat input more than 11.3 r/mm (sample 3 and 9), the tensile strength was slightly higher than the lowest standard value i.e. 180 MPa. If welds were without defects, a higher tensile strain was obtained.

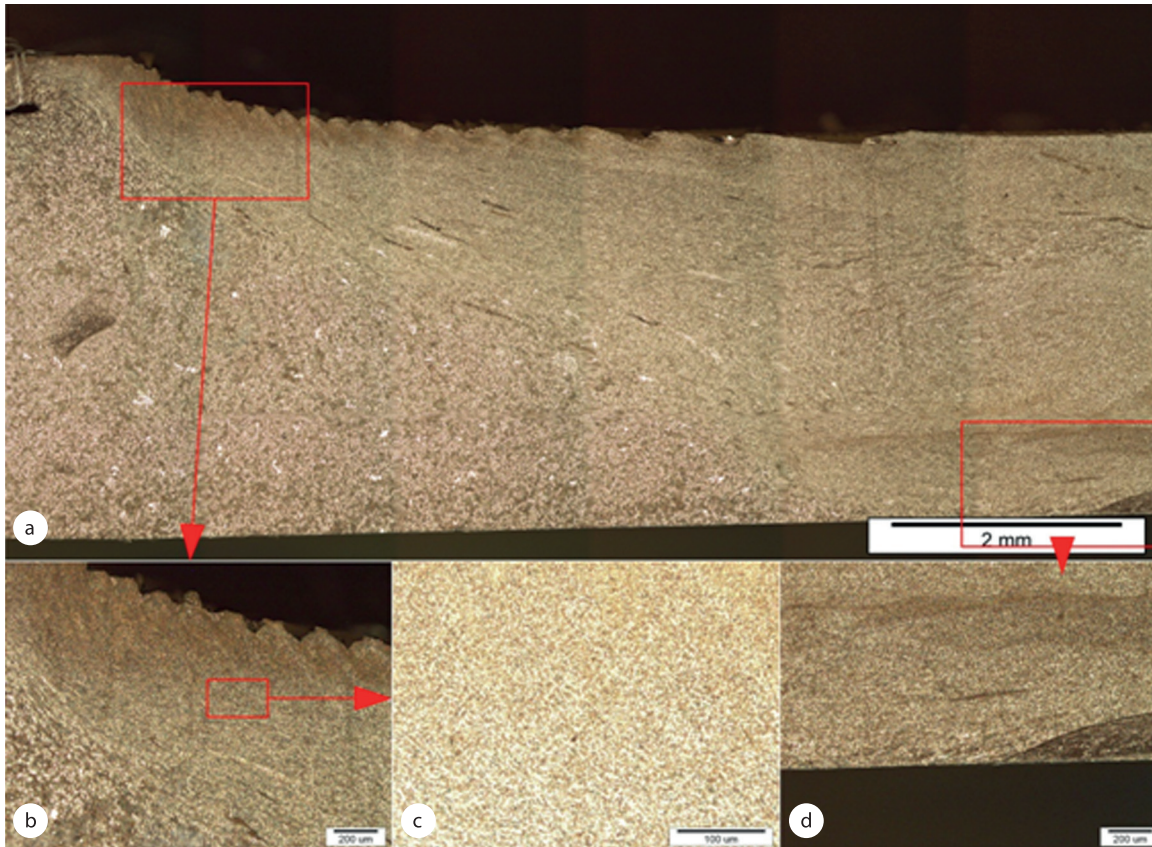


Figure 5: Microstructure (polarised light microscopy images) of FSW weld produced at 1 180 r/min RPF = 3.11 r/mm (sample 7): a) weld with HAZ and base alloy, b) weld apices and HAZ, c) weld and d) weld root.

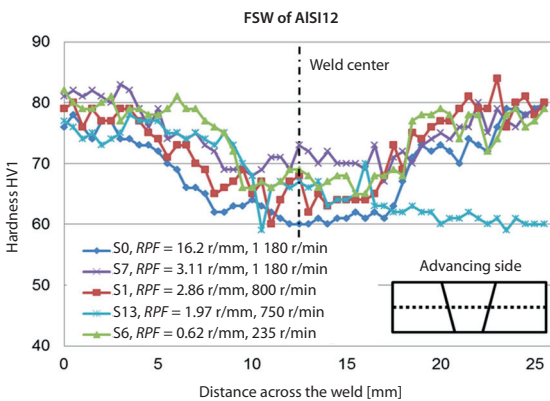


Figure 6: Weld hardness at different FSW parameters.

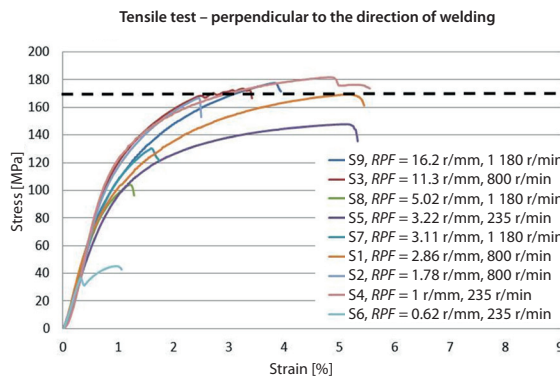


Figure 7: Results of tensile test.

Conclusions

Based on the analysed results the following can be summarized:

The tensile strength of the weld and base metal was similar in most cases. If the weld had a cavity, a low tensile strength was measured. Lower tensile strength than reference value was measured due to the porosity of base alloy, in which case the test sample broke in the base alloy and not in the weld. Tensile strength was in the range of base alloy, if the welds had no cavities, pores or other defects.

If $RPF < 1$ r/mm, an elongated cavity i.e. “worm hole” defect is present due to too low heat input. Quality welds (without cavities) are obtained if $RPF > 1$ r/mm ($FPR < 1$ mm/r). If RPF is high (> 5 r/mm) a toe flash and under-fill is possible due to high frictional heat input.

FSW welds had a finer microstructure compared to the base alloy, and were without pores even if the base alloy had them.

Welds were softer (60–70 HV1) compared to base alloy (80 HV1).

The friction coefficient changes with tool rotation speed. A higher heat input was noted at higher rpm at the same RPF/FPR rates.

Acknowledgements

The authors wish to thank Vinko Rotar, Gregor Humar, Uroš Braz, Nika Breskvar, and prof. dr. Ladislav Kosec for all the help at this research. The research was sponsored by Slovenian Research Agency under the grant L2-4183.

References

- [1] Feng, A. H., Ma, Z. Y. (2007): Enhanced mechanical properties of Mg–Al–Zn cast alloy via friction stir processing. *Scripta Materialia*, vol. 56, pp. 397–400.
- [2] Jana, S., Mishra, R. S., Baumann, J. A., Grant, G. (2010): Effect of process parameters on abnormal grain growth during friction stir processing of a cast Al alloy. *Materials Science and Engineering: A*, vol. 528, pp. 189–199.
- [3] Kim, Y. G., Fujii, H., Tsumura, T., Komazaki, T., Nakata, K. (2006): Effect of welding parameters on microstructure in the stir zone of FSW joints of aluminum die casting alloy. *Materials Letters*, vol. 60, pp. 3830–3837.
- [4] Kwon, Y. J., Shigematsu, I., Saito, N. (2008): Dissimilar friction stir welding between magnesium and aluminum alloys. *Materials Letters*, vol. 62, pp. 3827–3829.
- [5] Dobrzański, L. A., Reimann, L., Krawczyk, G. (2008): Influence of the ageing on mechanical properties of the aluminium alloy AlSi9Mg. *Archives of Materials Science and Engineering*, vol. 31, pp. 37–40.
- [6] Ma, Z., Sharma, S., Mishra, R. (2006): Effect of multiple-pass friction stir processing on microstructure and tensile properties of a cast aluminum–silicon alloy. *Scripta Materialia*, vol. 54, pp. 1623–1626.
- [7] Naiyi Li, T.-Y. P., Cooper, R. P., Houston, D. Q., Feng, Z., Santella, M. L. (2004): Friction stir welding of magnesium AM60 alloy. *Magnesium Technology*.
- [8] Nakata, K., Kim, Y. G., Fujii, H., Tsumura, T., Komazaki, T. (2006): Improvement of mechanical properties of aluminum die casting alloy by multi-pass friction stir processing. *Materials Science and Engineering: A*, vol. 437, pp. 274–280.
- [9] Santella, M. L., Engstrom, T., Storjohann, D., Pan, T. Y. (2005): Effects of friction stir processing on mechanical properties of the cast aluminum alloys A319 and A356. *Scripta Materialia*, vol. 53, pp. 201–206.
- [10] Uematsu, Y., Tozaki, Y., Tokaji, K., Nakamura, M. (2008): Fatigue behavior of dissimilar friction stir welds between cast and wrought aluminum alloys. *Strength of Materials*, vol. 40, pp. 138–141.
- [11] Ma, Z. R., Sharma, S. R., Mishra, R. S. (2006): Microstructural Modification of As-Cast Al–Si–Mg Alloy by Friction Stir Processing. *Metallurgical and Materials Transactions A*, 37A, pp. 3323–3336.
- [12] Lakshminarayanan, A. K., Balasubramanian, V. (2008): Process parameters optimization for friction stir welding of RDE-40 aluminium alloy using Taguchi technique. *Trans. Nonferrous Met. Soc. China*, vol. 18, pp. 548–554.
- [13] Properties of aluminium alloys, Aluselect [cited 2/25/2013]. Available on: <aluminium.matter.org.uk/aluselect/>.
- [14] H11 tool steel properties, Steel Selector Metal Ravne [cited 2/25/2013]. Available on: <www.metalravne.com/selector/selector.html>.